Inorganic Chemistry

Article

pubs.acs.org/IC

Magneto-optical Response of 3*d*-Decorated Polyoxomolybdates with *ε*-Keggin Structure

I. V. Andreev,[†] A. L. Tchougréeff,*[,†,‡,∇] P. Kögerler,[‡] and R. C. Rai[§]

[†]Department of Chemistry, Moscow State University, 119991 Moscow, Russia

[‡]Institut für Anorganische Chemie, RWTH−Aachen University, Landoltweg, 1, Aachen, D-52074, Germany

[∇]Poncelet Laboratory, Moscow Center for Continuous Mathematical Education, Moscow Independent University, 119002 Moscow, Russia

[§]Physics Department, Buffalo State College, 1300 Elmwood Avenue, Buffalo, New York 14222, United States

Supporting Information

ABSTRACT: A family of virtually isostructural tetra-capped *ε*-Keggin-type polyoxomolybdate(V) cluster compounds, $[Mo^{V}_{12}O_{28}(\mu^2{-}OH)_{10}(\mu^3{-}OH)_2\text{-}\{M^{II}(H_2O)_3\}_4]\cdot nH_2O$ ($\{M^{II}_4Mo^{V}_{12}\}$, M = Ni, Co), exhibits magnetic-field-dependent optical response in their electronic absorption spectra in the 0−33 T range. On the basis of Effective Hamiltonian Crystal Field calculations, we find that the observed field-induced decrease in reflectance of these compounds can be related to the formally spin-forbidden on-site *d*−*d* excitations. We tentatively position the observed effect among other known magneto-optical effects and predict that similar features may be found for other $\{M^{II}_4Mo^{V}_{12}\}$ analogues.

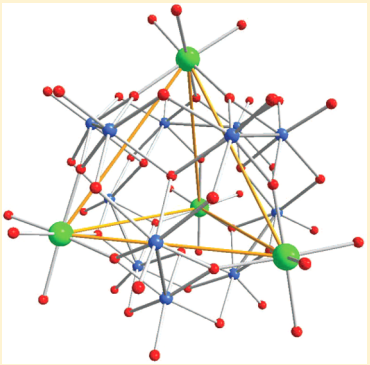

INTRODUCTION

Polyoxomolybdates provide a large set of diamagnetic scaffold structures that can be magnetically functionalized via integration of spin centers such as 3*d* transition-metal cations, resulting in spin clusters of unusual symmetries and connectivities exhibiting diverse magnetic characteristics, such as molecular spin frustration, spin-glass transitions, magnetic metastability, or charge-dependent exchange coupling.[1−3] A synthetic strategy in this context is based on the generation of highly nucelophilic polyoxoanions, which readily coordinate to cations via their structurally exposed oxygen positions. In the case of the reduction of buffered aqueous molybdate solutions by strong reducing agents such as hydrazine in the presence of Ni^{2+} or Co^{2+}, this results in the direct self-assembly of charge-neutral clusters of general composition $[Mo^{V}_{12}O_{28}(\mu^2{-}OH)_{10}\text{-}(\mu^3{-}OH)_2\{M^{II}(H_2O)_3\}_4]$ = $\{M_4Mo_{12}\}$, which crystallize as hydrates $\{M_4Mo_{12}\}\cdot nH_2O$ (n = 12−14).[4,5] The $\{M_4Mo_{12}\}$ cluster structures comprise the central almost T_d-symmetric *ε*-Keggin-type fragment, $[Mo^{V}_{12}O_{28}(\mu^2{-}OH)_{10}(\mu^3{-}OH)_2]^{8-}$, and four *fac*-$[M^{II}(H_2O)_3]$ groups coordinate each to three μ^2−O sites of the *ε*-Keggin cluster, defining an almost-regular M_4 spin tetrahedron. The Mo positions form six Mo^{V}_2 pairs with short Mo−Mo single bonds (<3 Å). The Mo−Mo single bonds result in spin pairing, which is directly evident from the diamagnetism of an analogous $\{Mo^{VI}_4Mo^{V}_{12}\}$-type cluster (even at 300 K), in which four (diamagnetic) $Mo^{VI}O_3$ groups occupy the positions of the $M^{II}(H_2O)_3$ groups in the $\{M_4Mo_{12}\}$ clusters.[7] In our two title compounds, superexchange between the M spin centers is mediated by −O−Mo−O− pathways, with average M···M distances of 6.6 Å.

The energy-dependent magneto-optical response of the Ni compound reveals an interesting structure slightly above the range of the allowed *d*−*d* excitations, which is our focus in this paper. To understand whether this is merely a feature of $\{Ni_4Mo_{12}\}$ or a manifestation of a more general effect, we synthesized the Co analogue and carried out similar experiments. Bringing our spectroscopy data on $\{Ni_4Mo_{12}\}$ and $\{Co_4Mo_{12}\}$ together with complementary calculations, we find that the magneto-optical response can be linked to formally spin-forbidden excitations of the *d*-manifold.

EXPERIMENTAL SECTION

Materials. The Ni- and Co-based $\{M^{II}_4Mo^{V}_{12}\}$ compounds have been prepared as previously described.[4,5] Their structure is depicted in Figure 1. We are currently working on the synthesis of other $\{M^{II}_4Mo^{V}_{12}\}$ derivatives, e.g., with M = Fe.

Optical and Magneto-optical Measurements. The optical response of pressed pellet samples of $\{Ni_4Mo_{12}\}$ and $\{Co_4Mo_{12}\}$ compounds was measured using a series of spectrometers, as described previously.[6] An open flow cryostat provided temperature control. The magneto-optics work was carried out at the National High Magnetic Field Laboratory in Tallahassee, FL, using a powered magnet.

Details of the Effective Hamiltonian Crystal Field (EHCF) Calculation. The Effective Hamiltonian Crystal Field (EHCF)

Received: October 21, 2013
Published: February 21, 2014

   dx.doi.org/10.1021/ic402645g | Inorg. Chem. 2014, 53, 2892−2898

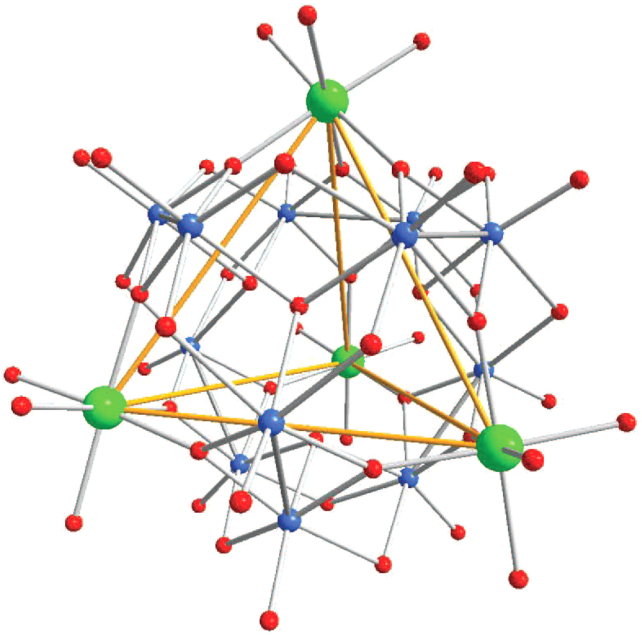

Figure 1. Molecular structure of $\{Ni_4Mo_{12}\}$ and $\{Co_4Mo_{12}\}$. Hydrogen atoms are omitted for the sake of clarity. Color code: Mo, blue; Ni/Co, green; and O, red. Orange lines highlight the tetrahedral M_4 substructure. See the Supporting Information for structure files (*xyz* format) for five different proton distribution patterns.

method used for theoretical estimates of the energies of *d*–*d* transitions is described in the literature.[8] We also give a brief summary of this method in section S1 in the Supporting Information, for the convenience of the readers. The Slater–Condon parameters for the Mo atoms were obtained from the Oleari's parameters,[9] and the core attractions and resonance parameters were taken from ref 10. All of the remaining parameters are either standard[8] or are modified, as is specified later.

The molecular geometries are known from the X-ray experiment only for the nickel and cobalt compounds.[4,5,11] Even they are uncertain up to positions of the protons. One can assume three types of the protons in these compounds: 24 of them are those of the 12 H_2O molecules coordinated to the capping M^{2+} ions. An additional 12 protons are distributed between the internal cavity and 12 bridging O atoms of the O–Mo_2–O groups. The presence of two H atoms inside the cavity is established for the isostructural $\{M_4^{VI}Mo_{12}^{V}\}$ compound.[7] We performed calculations for all five possible 2-vs-10 proton distributions.

The coordinates of the protons were restored as follows. The water molecules were put coordinated to the respective M^{2+} ions, so that the O atom had coordinates obtained from crystallographic data and the directions of the bisectors of the water HOH angles coincided with the $\overrightarrow{MO}$ vectors. The distances between the protons from different water molecules were controlled to be greater than 3 Å. The OH distances of the monoprotonated O atoms were set to be 1 Å. The angles ($\angle H(\mu_2\text{–}O)Mo$) were set to be 120°.

RESULTS AND DISCUSSION

Crystal Field Considerations. Considering the composition and the available structure information of the two title compounds, a first approach would be to interpret the observed spectra as those of the corresponding d^n ions in octahedral environments, i.e., equivalent to that of the hexahydrate complexes. In this case, $[Ni(H_2O)_6]^{2+}$ (ground state $^3A_{1g}$) shows two spin-allowed low-energy transitions at 8500 and 13 800 cm^{-1}, respectively, to the $^3T_{2g}$ and $^3T_{1g}$ states, whereas $[Co(H_2O)_6]^{2+}$ (ground state $^4T_{1g}$) shows three such transitions at 8100, ca. 16 000, and 19 400 cm^{-1} to the $^4T_{2g}$, $^4A_{2g}$, and $^4T'_{1g}$ states with the complication that the $^4A_{2g}$ transition, whose difference with $^4T_{2g}$ yields the key 10*Dq* value, is weak and thus cannot be positioned with sufficient precision. The interpretation of the spectrum of the Ni hexaaquacomplex is facile, the first transition yielding the value of 10*Dq* and the second being adequately reproduced with the value of the Racah parameter (*B*) recommended[14] for this compound (B = 930 cm^{-1}). Assuming the octahedral environment not to differ too much in the polyoxometallate cluster, two peaks are, in principle, expected in the reflectance spectrum, however, with somewhat-reduced average values of 10*Dq* and *B*, because of slightly larger Ni–O bond distances, compared to those in the hexahydrate and the nephelauxetic reduction, because of the presence of the polarizable ε-Keggin cage.[13] Unfortunately, the situation for Co is less clear. Even for $[Co(H_2O)_6]^{2+}$, the value[14] of 10*Dq* = 9200 cm^{-1}, which stems from ref 12, where the Jahn–Teller character of both the ground state and the first excited state is mentioned. This value seems to be an overestimate since it is clearly larger than the difference of 7900 cm^{-1} between the measured energies of the $\rightarrow^4T_{2g}$ and $\rightarrow^4A_{2g}$ transitions in the hexaaquacomplex, which, here, must be equal to 10*Dq*. It is also counterintuitive since the M–O bond length is larger in case of the hexaaquacobalt ion than in the case of the hexaaquanickel ion. [R(Co–O) = 2.09 Å, and R(Ni–O) = 2.06 Å. Data taken from Clack, D. W. and Farrimond, M. S. *J. Chem. Soc. A* **1971**, 2, 299.] However, using this value, together with the recommended[14] Racah parameter of B = 850 cm^{-1} leads to a very distorted description of the spectrum of $[Co(H_2O)_6]^{2+}$. In particular, the first transition occurs at too low energy (calcd. 6873 cm^{-1} vs measd. 8100 cm^{-1}) and the difference between $\rightarrow^4A_{2g}$ and $\rightarrow^4T'_{1g}$ transitions of ca. 4000 cm^{-1} instead of the observed 3400 cm^{-1}. The situation can only be partially improved by reducing the value of the Racah parameter *B*. If the latter is set to 750 cm^{-1}, then the calculated energy of the first transition becomes ca. 6920 cm^{-1} and the difference between $\rightarrow^4A_{2g}$ and $\rightarrow^4T'_{1g}$ amounts to 2500 cm^{-1}. This suggests a significant reduction in the Racah parameter *B* already in the Co hexaaquacomplex. Generally, *B* is the only free parameter controlling this part of the spectrum, under the condition that 10*Dq* is fixed at the measured energy difference between the $\rightarrow^4A_{2g}$ and $\rightarrow^4T_{2g}$ transitions. An agreement with the position of the first observed peak only very slowly improves with decreasing *B*, which, in turn, affects the relative position of the $\rightarrow^4A_{2g}$ and $\rightarrow^4T'_{1g}$ transitions.

Turning back to the uncomplicated case of the hexaaquanickel ion, modeling the behavior of the $\{Ni_4Mo_{12}\}$ compound, one immediately sees (see Table 1 in section S0 in the Supporting Information) both from the pure crystal field consideration and a simple EHCF calculations[16,17] that the formally spin-forbidden transition is located slightly above the higher of the two lowest allowed transitions. This is precisely where the depletion of the reflectance has been observed previously[6] for $\{Ni_4Mo_{12}\}$, which motivated the interpretation of the magneto-optical effect, as related to the spin-forbidden transitions. Applying this hypothesis to $\{Co_4Mo_{12}\}$ suggests that, because of the much-higher number of spin-forbidden transitions occurring between the spin-allowed ones, one can expect a more-structured spectrum of the magneto-optical response. However, a simplistic crystal field interpretation in this case seems to be insufficient, because of stronger geometry distortions occurring to the CoO_6 chromophores when

dx.doi.org/10.1021/ic402645g | *Inorg. Chem.* 2014, 53, 2892–2898

decorating the ε-Keggin than those of the NiO_6 chromophores. Thus, the EHCF calculations have been undertaken for the realistic geometries of the title compounds.

Optical Reflectance Spectra and Spin-Allowed Transitions. Reflectance measurements were previously performed[6] and presented as optical conductivity—a more-processed form—for the $\{Ni_4Mo_{12}\}$ compound. Here, we step back to the raw spectra and compare the results with our EHCF calculation (Figure 2). Analogously, in Figure 3, we represent

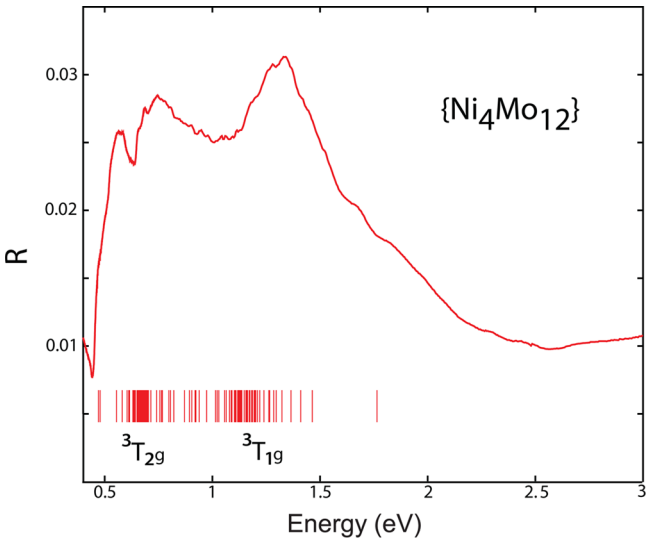

Figure 2. Optical reflectance (R) spectrum, as measured previously[6] at 7 K and compared with calculated allowed transition energies for four positions of the Ni^{2+} ions and five protonation patterns for the $\{Ni_4Mo_{12}\}$ compound.

the reflectance vs excitation energies data for the $\{Co_4Mo_{12}\}$ compound, as well in comparison with the EHCF calculated energies of the spin-allowed transitions.

The ground states of the Ni^{2+} ions in all four positions are $^3A_{2g}$. [Hereinafter, we use, for the electronic states, the symmetry notation with respect to the O_h group, which is an approximate symmetry of the local environment of each of the M^{2+} cations in the $\{M_4Mo_{12}\}$ compounds and the formal notation of the spin multiplicities derived from the model with a vanishing spin−orbit coupling. However, it should be understood that, in fact, the spatial multiplets are significantly split by the additional predominantly trigonal field stemming from the difference of the contributions to the effective crystal field as coming from three water molecules of the $[M^{II}(H_2O)_3]$ units and from the three μ^2−O sites of the ε-Keggin cluster coordinating these latter. The T_d-symmetry of the $\{M_4Mo_{12}\}$ clusters themselves is as well approximate so that the local geometries of the four distorted MO_6 octahedra are all somewhat different, which causes a difference in the transition energies of these four. To summarize, the ground-state notation $^3A_{2g}$ in the case of the Ni compound means nothing, but that it is the spin triplet with no closely lying states of the same spin. By contrast, the ground-state notation $^4T_{1g}$ for the Co compound reflects the fact that the numerical spin-quartet ground state is accompanied by two more closely lying quartets, as can be seen in section S3 in the Supporting Information.] Two reflectance peaks are assigned to the transitions to the respective groups of the $^3T_{2g}$ and $^3T_{1g}$ states stemming from the Ni^{2+} ions in slightly different coordination environments that

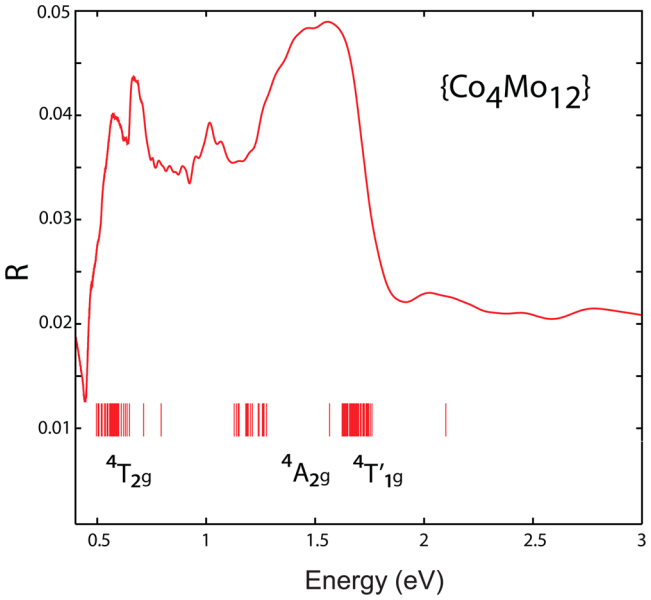

Figure 3. Optical reflectance (R) spectrum for the $\{Co_4Mo_{12}\}$ compound measured at 7 K, compared to the calculated allowed transition energies for four positions of the Co^{2+} ion five protonation patterns.

occur in each $\{M_4Mo_{12}\}$ cluster. The calculated energies (we slightly modified the Racah parameter B(Ni)—it is set to 830 cm^{-1}, compared to its value of 930 cm^{-1} in the corresponding hexaaqua complex—in order to reproduce the experimental reflectance spectrum of the Ni compound) are close to experimental ones, and generally there is no strong dependence on the protonation pattern. Only in the case of the II decoration position of the protonation pattern E (see section S3 in the Supporting Information and the file NiE.xyz available online), the effective crystal field felt by the corresponding d-shell turns out relatively strongly deformed, which manifests itself in the low-energy split from the $^3T_{2g}$ peak, which is observed well in Figure 2.

The measured optical reflectance spectrum of the $\{Co_4Mo_{12}\}$-compound, together with the predicted d−d transition energies is shown in Figure 3. The ground state, according to our calculations, is the $^4T_{1g}$ state. Because of the stronger deformation of the CoO_6 chromophores, ascribing the spectral structure directly to the crystal field states of octahedrally coordinated Co^{2+} ions may be too simplistic. The plausible interpretation of the smaller, but distinct peak at ca. 8000 cm^{-1} (ca. 1 eV) in the reflectance spectrum of the $\{Co_4Mo_{12}\}$ compound as $\rightarrow{}^4A_{2g}$ transition may be misleading, since it implies an unrealistically small value of average 10Dq of ca. 3000 cm^{-1}. Following the suggestion[14] that $\rightarrow{}^4A_{2g}$ transitions are weak and appear largely as shoulders of the stronger $\rightarrow{}^4T'_{1g}$ line at ca. 12 000 cm^{-1} (ca. 1.5 eV), we estimate the average 10Dq as 6000−7000 cm^{-1}, which is confirmed by our direct calculation shown in Figure 3 and in section S3 in the Supporting Information. If the standard (free ion) Racah parameters[8] are used, the spin-allowed transition $\rightarrow{}^4T'_{1g}$ becomes of a higher energy than the highest reflection band observed in the experiment. We previously discussed the reasons why the Racah parameter B(Co) must be reduced already in the hexahydrate. However, the Racah parameters B(Co) and C(Co) do further change in the polarizable polyoxometallate environment, because of the nephelauxetic

dx.doi.org/10.1021/ic402645g | Inorg. Chem. 2014, 53, 2892−2898

effect.[12,13] Taking this into account allows us to reproduce the experimental spectrum by fixing the Racah parameter $B(Co)$ = 650 cm^{-1}. In this case, the energy for the $^4T_{1g} \rightarrow {}^4T'_{1g}$ transition in the $\{Co_4Mo_{12}\}$ compound amounts to ca. 12 000−13 000 cm^{-1} (1.5−1.6 eV), which fairly accurately corresponds to the strongest observed peak in the reflectance spectrum shown in Figure 3. This nephelauxetic renormalization of the Racah parameter can be attributed, in principle, to the presence of an easily polarizable, all-Mo(V) ε-Keggin cluster responsible for a stronger nephelauxetic effect.[13] A similar amount of this effect is observed in the Ni compound (see above).

Generally, one can consider the agreement between the observed features in the $\{M_4Mo_{12}\}$ series to be reasonable.

Magneto-optic Response and Spin-Forbidden Transitions. The main goal of this work is to tentatively interpret the magneto-optic effect previously observed in the $\{Ni_4Mo_{12}\}$ compound[6] and to learn whether it is an isolated feature or a more general one. Thus, we recorded the reflectance spectra in an applied field of up to 33 T and calculated the ratio of the reflectance measured in the field to reflectance measured in zero field (hereinafter referred to as the reflectance ratio). That for the $\{Ni_4Mo_{12}\}$ compound is presented in Figure 4. It is

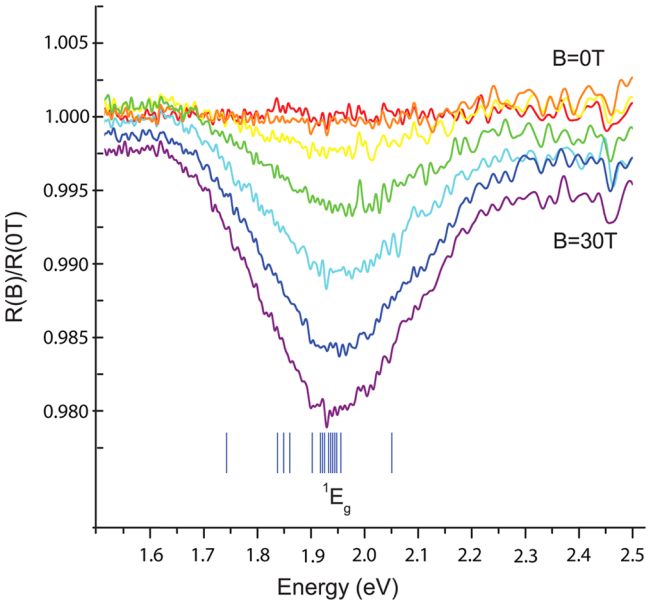

Figure 4. Reflectance ratio spectra of the $\{Ni_4Mo_{12}\}$ compound,[6] compared to the calculated energies of the forbidden d−d transitions for four positions of the Ni^{2+} ions and five protonation patterns.

remarkable that the single feature, rather broad band, of this spectrum occurs well above the upper band of the spectrum of the reflectance itself (Figure 2). Considering the d−d excitation spectrum of the $[Ni(H_2O)_6]^{2+}$ ion either experimental[14] or calculated[16,17] by the EHCF method[8] we found that the spin-forbidden $^3A_{2g} \rightarrow {}^1E_g$ transition occurs in the energy range right above the allowed d−d transitions. Thus, we undertook the respective calculation of the forbidden $^3A_{2g} \rightarrow {}^1E_g$ transitions for the four Ni^{2+} ions of the $\{Ni_4Mo_{12}\}$ compound. The results are shown in Figure 4.

We find a remarkable agreement between the calculated energies of the $^3A_{2g} \rightarrow {}^1E_g$ transitions and the position of the band in the reflectance ratio spectra. This allows us to formulate a hypothesis, that the reflectance depletion observed in the strong magnetic field occurs due to a magnetic field induced intensity redistribution between the spin-allowed and spin-forbidden d−d transitions.

With this hypothesis in mind, we performed further measurements of the reflectance ratio spectra for the $\{Co_4Mo_{12}\}$ compound as well in comparison with the EHCF-calculated energies of the spin-forbidden transitions. As evident from the results shown in Figure 5, the situation in the $\{Ni_4Mo_{12}\}$ compound is by no means unique and much richer reflectance ratio spectra can be observed for the $\{Co_4Mo_{12}\}$ analogue.

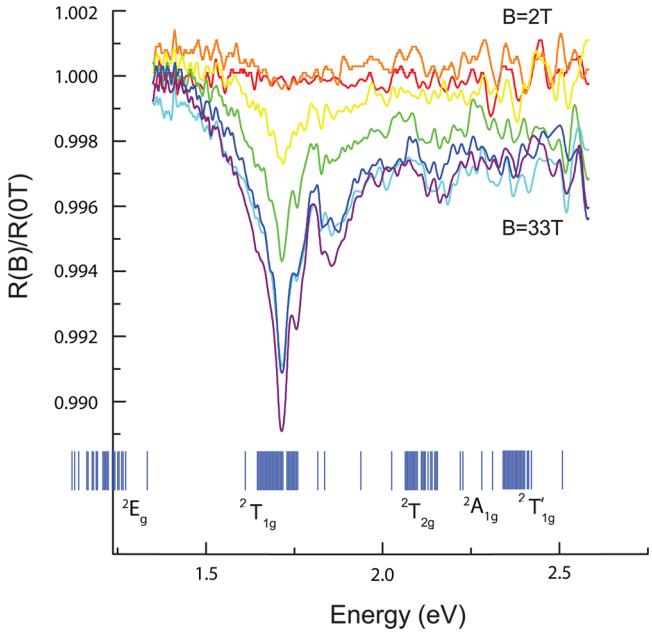

Figure 5. Reflectance ratio spectra of the $\{Co_4Mo_{12}\}$ compound, compared to the calculated energies of the forbidden d−d transitions for four positions of the Co^{2+} ions and five protonation patterns.

The reflectance ratio spectrum of the $\{Co_4Mo_{12}\}$ compound contains many more features than that of the $\{Ni_4Mo_{12}\}$ compound. This is in agreement with the general crystal field theory prediction concerning the number of the states of different spin and symmetry. Correspondingly, one can expect the following spin-forbidden transitions for the Co^{2+} ion: $^4T_{1g} \rightarrow {}^2E_g$, $\rightarrow {}^2T_{1g}$, $\rightarrow {}^2T_{2g}$, $\rightarrow {}^2A_{1g}$, and $\rightarrow {}^2T'_{1g}$. The energy of the first forbidden transition is ∼8000 cm^{-1} and does not fall into the range studied for the magneto-optical response. On the basis of calculations of the hexahydrate complex $[Co(H_2O)_6]^{2+}$, which, as in the case of the Ni compound, serves as a simplest approximate model of the corresponding $\{M_4Mo_{12}\}$ species one could expect magneto-optical features at the energies of ca. 9000, 14 000, 17 000, and 20 000 cm^{-1} (ca. 1.12, 1.73, 2.11, and 2.5 eV). The energies of the two highest transitions $\rightarrow {}^2A_{1g}$ and $\rightarrow {}^2T'_{1g}$ are almost degenerate in the hexahydrate complex, thus resulting in a single feature in the reflectance ratio spectrum.

Our calculations performed for the crystallographically determined geometry of the $\{Co_4Mo_{12}\}$ cluster predict some magneto-optic effect, because of the $\rightarrow {}^2E_g$ transition at an energy of ∼8000 cm^{-1} (1 eV). However, it can be masked by the strong allowed transitions seen in Figure 3 in that spectral range. The strongest reflectance ratio band at the energy of 14 000 cm^{-1} (1.74 eV) is tentatively attributed to the $\rightarrow {}^2T_{1g}$ transition, its twin peak refers then to the $\rightarrow {}^2T_{2g}$ transition, the higher energy features at ca. 18 000 cm^{-1} (ca. 2.23 eV) is then

dx.doi.org/10.1021/ic402645g | Inorg. Chem. 2014, 53, 2892−2898

the $\rightarrow^2A_{1g}$ transition, whereas the highest energy features at ca. 21 000 cm^{-1} (ca. 2.55 eV) refer to the $\rightarrow^2T'_{1g}$ one. We see that the $\rightarrow^2A_{1g}$ and $\rightarrow^2T'_{1g}$ almost degenerate in the hexahydrate complex split apart at the lower (average) values of $10Dq$ and B characteristic for the $\{Co_4Mo_{12}\}$ compound. However, one must not take the symmetry labeling too rigorously, because of significant geometry distorsions characteristic for the $\{Co_4Mo_{12}\}$ cluster. We can conclude that the initial hypothesis concerning the attribution of the bands in the reflectance ratio spectra to the spin-forbidden $d-d$ transitions is consistent with the spectra of the $\{Co_4Mo_{12}\}$ compound.

One may wonder how it is possible that the magneto-optic effect we observe manifests as a depletion of the intensity of already forbidden transitions. To clarify this point, we remind that we use for the electronic states the symmetry notation with respect to the O_h group, which is an approximate symmetry of the local environment of each of the M^{2+} cations in the $\{M_4Mo_{12}\}$ compounds and the formal notation of the spin multiplicities derived from the model with a vanishing spin–orbit coupling. In fact, all the approximate symmetries used for the states' labeling are broken. Thus, none of the selection rules (neither the Laporte evennes rule nor the spin-conservation rule) for the electric dipole transitions are strictly obeyed. This is the reason why either optical or magneto-optical signal appears in the entire studied energy range. In this situation, the distinction between "allowed" and "forbidden" transitions is a matter of labeling these latter rather than the substance. That is to say that, in reality, all the discussed transitions are effectively allowed and the applying the field results only in redistribution of the intensity between these transitions.

An Attempt to Classify the Observed Magneto-optical Effect: To MOKE or Not To MOKE? The magneto-optical measurements[6] together with those performed in the present paper suggest that the observed depletions of the reflectance at the energies of the formally spin-forbidden $d-d$ transitions occurring in a strong applied magnetic field represent a general phenomenon, may be even not restricted by the particular class of the molecules, where it has been observed for the first time. Thus, in the present section, we try to position it among other fairly versatile magneto-optical effects differing by the specific of the setting geometry (mutual orientation of the sample, incident and outcoming light beams, direction of the applied field, etc.) and by this to establish prerequisites for future development of the model of this seemingly new effect. It apparently shows up as a depletion in the reflectance spectra resembling the Fano antiresonances as they are described in, e.g., ref 18, where such narrow deeps are indeed observed within a broad allowed transition. Our effect appears differently: the magneto-optic features in both compounds do not appear among the allowed transitions, but rather above the allowed transitions. This manifests in the applied field—no depletion occurs without field—as it was in the papers;[18] thus, these are not Fano antiresonances.

The geometry of the magneto-optical measurements[6] and those reported in this paper is depicted in Figure 6. This setting is characteristic for studying the magneto-optical Kerr effect in the polar version: reflection mode (in our case almost normal incidence) and magnetic field set normal to the sample surface.[19] An important difference to other magneto-optical effects of the mentioned class is that those are observed for polarized light and manifest themselves in rotation of the polarization plane of the reflected beam, relative to that of the incident beam for the linearly polarized light and/or appearance

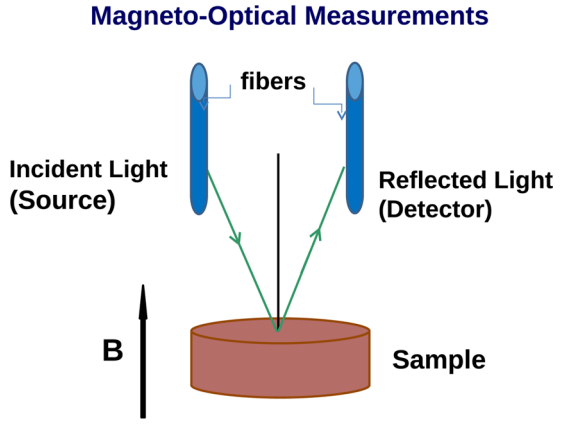

Figure 6. Experimental setting for the magneto-optical measurements. The angle between the incident and reflected beams (green lines with arrows) is twice the incidence angle (ϕ_i).

of the ellipticity and field dependency of the directions of the axes of the ellipses in the reflected beam for the circularly polarized incident beams. Similar to magnetic circular dichroism (MCD),[20] the magneto-optic response observed previously[6] and in the present paper manifests itself in the dependence of the intensity of the reflected light both on the applied field and on the frequency/energy. In contrast to MCD, in our case, the effect is observed for nonpolarized light (because of the use of polycrystalline powder samples).

As we show in detail in section S2 in the Supporting Information, where definitions of the basic relevant (magneto-)optical quantities also are derived, the expression for the reflectance ratios shown in Figures 4 and 5 reads:

$$\frac{R(\omega, \mathcal{B})}{R(\omega, 0)} - 1 = 2\mathcal{R}\frac{\delta\chi_{xx}(\omega, \mathcal{B})}{\chi_{xx}(\omega, 0)} + \frac{|\chi_{xy}(\omega, \mathcal{B})|^2}{|\chi_{xx}(\omega, 0)|^2} \quad (1)$$

where $\chi_{\mu\nu}$ are the Cartesian components of the electric polarizability tensor, $\delta\chi_{xx}$ is the field-induced variation of the respective component of that tensor, and $\mathcal{R}$ stands for the real part of the subsequent expression; $\mathcal{B}$ is the applied magnetic field. The second term in eq 1 is always positive, so that the observed values of the reflectance ratio (less than unity) must be attributed to a decrease of the diagonal element of the dielectric tensor at the frequency of a formally spin-forbidden transition in the applied magnetic field. Since the Hall conductivity tensor (ultimately contributing the off-diagonal component of the electric polarizability tensor, χ_{xy}) is odd, with respect to the applied magnetic field (changes its sign when the direction of the applied field is reverted since the direction of the Hall current inverts under the same revertion), its lowest-order expansion term, with respect to the applied field, can be only linear with respect to $\mathcal{B}$. By contrast, the normal conductivity tensor (and thus the diagonal part of the electric polarizability tensor χ_{xx}) does not change its sign when the magnetic field is reverted (the direction of the normal current remains the same when the applied field reverts); it is thus an even function of $\mathcal{B}$ and, thus, its expansion cannot start at any power lower than the second power, with respect to the applied field. Thus, $\delta\chi_{xx}(\omega, \mathcal{B})$ cannot be lower than the second power in $\mathcal{B}$ either.[19,21] Although the effects linear with respect to $\mathcal{B}$ and dependent on the off-diagonal element of the dielectric tensor χ_{xy} are well-known (the polar Kerr effect itself, for example), under the present experimental setting, these terms

dx.doi.org/10.1021/ic402645g | Inorg. Chem. 2014, 53, 2892–2898

appear to be dependent on $\mathcal{B}^2$ (due to the squared absolute value in eq 1).

Following the estimates of the strength of various electro-/magneto-optical effects,[21] the squared magnitude of the effects linear in $\mathcal{B}$ (the second term in eq 1) is at least 2 orders of magnitude smaller than that of the contributions to $\delta\chi_{xx}(\omega, \mathcal{B})$, which are intrinsically dependent on $\mathcal{B}^2$. The magneto-optical responses, quadratic with respect to the applied magnetic field, are the well-known Voigt or (in the case of condensed samples) Cotton−Mouton effects. They are manifested in the transmission setting as a modification of polarized light being dependent on the off-diagonal element of the dielectric tensor. As for the second-order $\mathcal{B}$ dependence of the diagonal element of the dielectric tensor $\delta\chi_{xx}(\omega, \mathcal{B})$, such effects have been reported and the name of quadratic magneto-optic Kerr effect (QMOKE) has been coined for them.[22,23] However, the experimental settings,[22,23] are designed to follow the features of the polarized light (polarization plane rotation and ellipticity angles), which are, by far, more spectacular than the intensity variation observed in our setting, although observed at a single value of the light frequency. Nevertheless, only a detailed microscopic theory, which seems yet to be developed, will be able to give substantiated estimates of the magnitude of this effect.

CONCLUSION

By extending the magneto-optical study—namely, the magnetic field dependence of visible/near-infrared (vis-NIR) reflectance spectra—to the Co member of the family of the $\{M_4Mo_{12}\}$-polyoxometallate compounds with the ε-Keggin structure, we demonstrate that the previously observed findings on the Ni-member of this family are not isolated. Both compounds exhibit a complex magneto-optical response in fields up to 33 T at energies characteristic for formally spin-forbidden $d-d$ transitions. Our experimental results are rationalized by a systematic computational study of the electronic structure of the $\{M_4Mo_{12}\}$ compounds with M = Ni, Co performed with use of the EHCF method.[8] Our numerical analysis adequately reproduces the positions of the peaks in the reflectance spectrum without external field by identifying them with the energies of the allowed $d-d$ transitions. The magneto-optic response in the reflectance ratio spectra is thus attributed to the *formally* spin-forbidden transitions. The spin-forbidden transitions with a total spin variation of 1 manifest themselves as depletions of the reflectance in the external field, most probably proportional to the square of the applied field. Although the magnitude of the observed magneto-optic effects and their precise nature deserve additional consideration, we conclude that, with reasonable allowances to the uncertainties in geometries, the qualitative agreement between calculated and experimental spectra in terms of the positions of the reflectance-ratio bands is achieved.

ASSOCIATED CONTENT

Supporting Information

Brief descriptions of the Crystal Field-based analysis of the title compounds (section S0), the EHCF method used[8] (section S1), the reference information concerning magneto-optical effects (section S2), the lower-energy segments of the EHCF calculated spectra of the decorating transition metal ions in four positions in the ε-Keggin structures for five protonation patterns (section S3), and the EHCF input files for all performed calulations (section S4) is provided, as well as the *.xyz files of the molecular geometries of the title compounds in all five cage protonation patterns. This material is available free of charge via the Internet at http://pubs.acs.org.

AUTHOR INFORMATION

Corresponding Author

*E-mail: andrei.tchougreeff@ac.rwth-aachen.de.

Notes

The authors declare no competing financial interest.

ACKNOWLEDGMENTS

We acknowledge the Russian Foundation for Basic Research for the financial support extended to the group at the Poncelet Lab (through Grants Nos. 10-03-00155 and 14-03-00867). Prof. J. L. Mustfeldt (Department of Chemistry, University of Tennessee, Knoxville) is acknowledged for helpful discussions and suggestions. The Referees are acknowledged for comments which helped to improve the manuscript.

REFERENCES

(1) Kögerler, P.; Tsukerblat, B.; Müller, A. *Dalton Trans.* **2010**, *39*, 21.

(2) Ritchie, C.; Ferguson, A.; Nojiri, H.; Miras, H. N.; Song, Y.-F.; Long, D.-L.; Burkholder, E.; Murrie, M.; Kögerler, P.; Brechin, E. K.; Cronin, L. *Angew. Chem., Int. Ed.* **2008**, *47*, 5609.

(3) Botar, B.; Ellern, A.; Hermann, R.; Kögerler, P. *Angew. Chem., Int. Ed.* **2009**, *48*, 9080.

(4) Ellern, A.; Kögerler, P. *Acta Crystallogr., Sect. C: Cryst. Struct. Commun.* **2012**, *68*, 17.

(5) Müller, A.; Beugholt, C.; Kögerler, P.; Bögge, H.; Bud'ko, S.; Luban, M. *Inorg. Chem.* **2000**, *39*, 5176.

(6) Schnack, J.; Brüger, M.; Luban, M.; Kögerler, P.; Morosan, E.; Fuchs, R.; Modler, R.; Nojiri, H.; Rai, R. C.; Cao, J.; Musfeldt, J.; Wei, X. *Phys. Rev. B.* **2006**, *73*, 094401.

(7) Khan, M. I.; Müller, A.; Dillinger, S.; Bögge, H.; Chen, Q.; Zubieta, J. *Angew. Chem., Int. Ed. Engl.* **1993**, *32*, 1780.

(8) Soudackov, A. V.; Tchougréeff, A. L.; Misurkin, I. A. *Theor. Chim. Acta* **1992**, *83*, 389; the package implementing the used EHCF method is available for calculations to the registered users of the NetLaboratory at http://www.qcc.ru/~netlab/, entry EHCF2.5.

(9) di Sipio, L.; Tondello, E.; de Michelis, G.; Oleari, L. *Chem. Phys. Lett.* **1971**, *11*, 287.

(10) Ruette, F.; Valencia, N.; Sanchez-Delgado, R. *J. Am. Chem. Soc.* **1989**, *111*, 40.

(11) Furrer, A.; Krämer, K. W.; Strässle, T.; Biner, D.; Hauser, J.; Güdel, H. U. *Phys. Rev. B* **2010**, *81*, 214437.

(12) Jørgensen, C. K. *Adv. Chem. Phys.* **1963**, *5*, 33; *Prog. Inorg. Chem.* **1964**, *4*, 73.

(13) Tchougréeff, A. L.; Dronskowski, R. *Int. J. Quantum Chem.* **2009**, *109*, 2606.

(14) Lever, A. B. P. *Inorganic Electronic Spectroscopy*; Elsevier: Amsterdam, 1984.

(15) Sviridov, D.; Smirnov, Y. *Theory of Optical Spectra of Transition-Metal Ions* (in Russ.); Nauka: Moscow, 1977.

(16) Soudackov, A. V.; Tchougréeff, A. L.; Misurkin, I. A. *Zh. Fiz. Khim.* **1994**, *68*, 1256 (in Russ.).

(17) Tokmachev, A. M.; Tchougréeff, A. L. *Khim. Fiz.* **1999**, *18*, 80 (in Russ.).

(18) Rodriguez-Mendoza, U. R.; Rodriguez, V. D.; Lavin, V.; Martin, I. R.; Nunez, P. *Spectrochim. Acta A* **1999**, *55*, 1319. Lempicki, A.; Andrews, L.; Nettel, S. J.; McCollum, B. C.; Solomon, E. I. *Phys. Rev. Lett.* **1980**, *44*, 1234.

(19) Oppeneer, P. M. Magneto-optical Kerr Spectra. In *Handbook of Magnetic Materials*, Vol. *13*; Buschow, K. H. J., Ed.; Elsevier: Amsterdam, 2001; pp 229−422.

(20) (a) Buckingham, A. D.; Stephens, P. J. *Annu. Rev. Phys. Chem.* **1966**, *17*, 399. (b) Barron, L. D.; Vrbancich, J. *Mol. Phys.* **1984**, *51*, 715.
(21) (a) Baranova, N. B.; Bogdanov, Y. V.; Zel'dovich, B. Y. *Usp. Fiz. Nauk [Sov. Phys. Usp.]* **1977**, *123*, 349. (b) Baranova, N. B.; Zel'dovich, B. Y. *Mol. Phys.* **1979**, *38*, 1085.
(22) Hamrle, J.; Blomeier, S.; Gaier, O.; Hillebrands, B.; Schneider, H.; Jakob, G.; Postava, K.; Felser, C. *J. Phys. D: Appl. Phys.* **2007**, *40*, 1563.
(23) Muduli, P. K.; Rice, W. C.; He, L.; Collins, B. A.; Chu, Y. S.; Tsui, F. *J. Phys.: Condens. Matter.* **2009**, *21*, 296005.
(24) Harrison, W. A. *Electronic Structure and the Properties of Solids*, W. H. Freeman and Company: San Francisco, CA, 1990; Chapter 19.
(25) (a) Georges, A.; Kotliar, G.; Krauth, W.; Rozenberg, M. J. *Rev. Mod. Phys.* **1996**, *68*, 13. (b) Held, K.; Nekrasov, I. A.; Keller, G.; Eyert, V.; Blümer, N., McMahan, A. K.; Scalettar, R. T.; Pruschke, T.; Anisimov, V. I.; Vollhardt, D. *Quantum Simulations of Complex Many-Body Systems: From Theory to Algorithms*, Lecture Notes, NIC Series, No. 10; Grotendorst, J., Marx, D., Muramatsu, A., Eds.; John von Neumann Institute for Computing (NIC): Jülich, Germany, 2002; p 175.
(26) Schäffer, C. E.; Jørgensen, C. K. *Mol. Phys.* **1965**, *9*, 401.
(27) You, C.-Y.; Shin, S.-C. *Appl. Phys. Lett.* **1996**, *69*, 1315.
(28) Qiu, Z. Q.; Bader, S. D. *Rev. Sci. Instrum.* **2000**, *71*, 1243.